Journal of ELECTRONIC MATERIALS, Vol. 37, No. 2, 2008 *Regular Issue Paper*
DOI: 10.1007/s11664-007-0319-x
© 2007 TMS

Ball Impact Responses of Ni- or Ge-Doped Sn-Ag-Cu Solder Joints

YI-SHAO LAI,[1,3] JENN-MING SONG,[2] HSIAO-CHUAN CHANG,[1] and YING-TA CHIU[1]

1.—Central Labs, Advanced Semiconductor Engineering, Inc., 26 Chin 3rd Rd., Nantze Export Processing Zone, 811 Nantze, Kaohsiung, Taiwan. 2.—Department of Materials Science and Engineering, National Dong Hwa University, Hualien 974, Taiwan. 3.—e-mail: yishao_lai@aseglobal.com

In this work, we present ball impact test (BIT) responses and fractographies obtained at an impact velocity of 500 mm/s on Sn-4Ag-0.5Cu, Sn-1Ag-0.5Cu, Sn-1Ag-0.5Cu-0.05Ni, Sn-1.2Ag-0.5Cu-0.05Ni, and Sn-1Ag-0.5Cu-0.05Ge package-level solder joints. The solder joints are bonded on substrate pads of either immersion tin (IT) or direct solder on pad (DSOP) surface finishes. Differences of BIT results with respect to multi-reflow are also reported. Taking the impact energy as an indication of board-level drop reliability of the solder joints, the BIT results indicate that better reliability can be achieved by adopting Sn-Ag-Cu solder alloys with low Ag weight contents as well as IT substrate pad finish rather than DSOP. Moreover, the addition of Ni or Ge to the solder alloy provides a large improvement; Ni alters the interfacial intermetallic compound (IMC) structure while Ge enhances the mechanical behavior of the bulk solder.

Key words: Ball impact test (BIT), solder joint, substrate pad surface finish, board-level drop reliability

INTRODUCTION

The ball impact test (BIT), or so-called high-speed ball shear test, was developed based on the demand of a package-level measure of board-level reliability of solder joints[1,2] in the sense that it leads to brittle fracturing around the interfacial intermetallic compound (IMC), similar to that from a board-level drop test.[3–5] Development of several BIT apparatuses has been reported in recent years.[1,2,6–10] To date, the majority of BIT studies have presented only failure-mode statistics because the specific test apparatuses employed in these studies might not allow accurate measurements of force and displacement responses induced by the impact load. The BIT apparatus has to be properly designed to measure reasonable impact force profiles generated during BIT at a high impact velocity.[11] The characteristics of an impact force profile represent scientifically meaningful factors when correlating with board-level drop reliability and indeed a positive correlation has been found empirically between these BIT characteristics and the board-level drop reliability of electronic packages.[1,2] In addition to the development of BIT apparatuses, numerical studies of the BIT process that provide insights into the transient mechanical behavior of the solder joint have been carried out by Yeh and coworkers.[12–15] Besides the intention to correlate with board-level drop reliability, BIT also stands alone as a unique and novel test methodology for the characterization of the strengths of solder joints under a high-speed shearing load.

Numerous studies have been devoted to examining the effect of Ag contents and microelement additions on the properties of Sn-Ag-Cu solder alloys. Among Sn-xAg-0.5Cu (x = 1, 2, 3, and 4) flip-chip solder joints, 3% Ag shows excellent fatigue performance under a broad range of strain

(Received June 19, 2007; accepted October 8, 2007; published online October 30, 2007)

conditions. On the other hand, solder joints with 1% Ag exhibit superior fatigue endurance only when a high plastic strain is present.[16] Kariya et al.[17] suggested that a very small amount of Ni addition (0.05 wt.%) can enhance the fatigue endurance of 1%Ag flip-chip solder joints so that their performance becomes comparable to that of 3%Ag solder joints. It has been reported that, in the case when the Sn-3.5Ag-0.07Ni solder alloy was bonded onto Cu, the interfacial IMC was irregular worm-like $(Cu,Ni)_6Sn_5$ rather than scalloped Cu_6Sn_5 and its thickness did not appear to change after long-time aging.[18] Also, the addition of a small amount of Ge can effectively reduce dross, raise the mechanical strength, and improve the thermal fatigue resistance of solder joints.[19]

To date, however, the effect of the addition of microelements on the BIT responses of Sn-Ag-Cu solder joints has not been investigated systematically. In this work, we present BIT responses measured at an impact velocity of 500 mm/s on Sn-4Ag-0.5Cu, Sn-1Ag-0.5Cu, Sn-1Ag-0.5Cu-0.05Ni, Sn-1.2Ag-0.5Cu-0.05Ni, and Sn-1Ag-0.5Cu-0.05Ge package-level solder joints. The solder joints were bonded on substrate pads of either immersion tin (IT) or direct solder on pad (DSOP) surface finish. Differences of BIT results with respect to three-time reflow are also reported.

BALL IMPACT TEST

The Instron MicroImpact testing system (Instron Ltd., Buckinghamshire, UK) was employed in this study for BIT tests. For each BIT test, a striker was catapulted upon release of an air-compressed spring with an impact velocity, V_i, of up to 1 m/s. The impact process was therefore energy controlled, although the impact velocity changed slightly during the course of impact. A typical impact force profile[2] measured by the BIT apparatus is shown in Fig. 1. The impact force increases after the pin hits the solder joint and then decreases after fracturing in the solder joint is initiated.[12–14] Since the post-failure structural behavior of the solder joint is extremely complicated and hardly reproducible, we consider only the ascending part of the first peak of the impact force profile, which represents the structural behavior of the solder joint from the initiation of the impact load until fracturing starts.

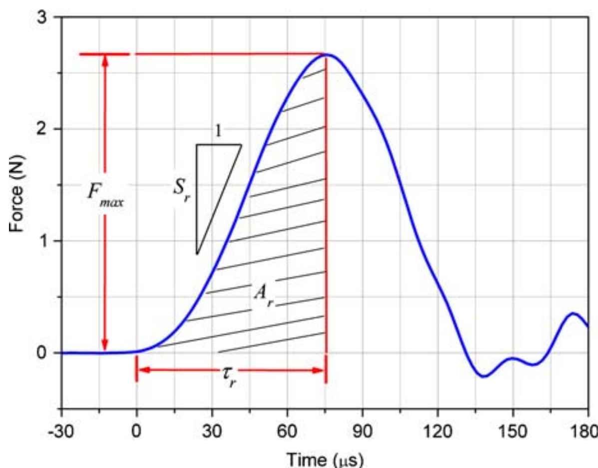

Fig. 1. Typical measured impact force profile.[2]

The characteristics of the impact force profile are depicted in and derived from Fig. 1 as follows. F_{max} is the peak impact force. For the IMC fracturing failure mode, F_{max} corresponds to the IMC strength, which is a mix of the normal and shear adhesion strengths of the solder joint because BIT actually applies mixed-mode loading to the solder joint.[12–14] τ_{r} denotes the duration of the ascending part of the impact force profile. If V_{i} varies insignificantly during the entire impact process, we have $\delta \cong V_{\mathrm{i}} \times \tau_{\mathrm{r}}$, where δ stands for the traveling distance of the striker from the onset of the impact until the initiation of fracturing in the solder joint. Either τ_{r} or δ can be used as a measure of the ductility of the solder joint. A_{r} is the area below the ascending part of the impact force profile, which represents the toughness of the solder joint. This quantity is proportional to the impact energy exerted during the ascending part, E_{r}, because if V_{i} varies insignificantly during the entire impact process, we have $E_{\mathrm{r}} \cong V_{\mathrm{i}} \times A_{\mathrm{r}}$. The S_{r} is the slope of the ascending part of the impact force profile. If V_{i} varies insignificantly during the entire impact process, we have $S_{\mathrm{r}} \cong V_{\mathrm{i}} \times K_{\mathrm{r}}$, where K_{r} is the apparent stiffness of the solder joint structure.

Typical BIT-induced failure modes are illustrated in Fig. 2: mode C denotes fracturing within the solder alloy, mode B represents fracturing around the interfacial IMC layer, and mode B1 stands for pad peeling. A mixed failure mode is frequently observed in actual tests such that part of the fractured surface features IMC fracturing, which in general is the initial failure, while the remainder is covered by solder residues, a result of post-failure crack propagations. Since only the ascending part of the impact force profile is of interest, and the solder joint remains intact until the peak impact force is reached,[12–14] this mixed failure mode is regarded as mode B.

In this study, ten sets of ball grid array (BGA) samples were prepared; the experiment cells are tabulated in Table I. These experiment cells were

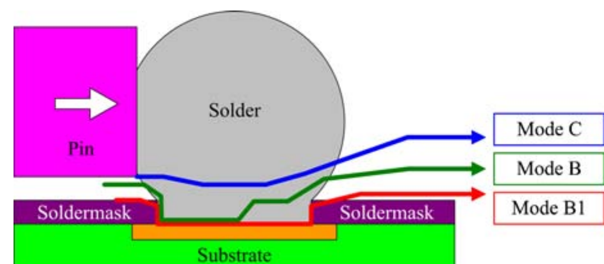

Fig. 2. Typical BIT-induced failure modes.

Table I. Experimental Cells

Cell	Solder Composition	Pad Finish
A	Sn-4Ag-0.5Cu	IT or DSOP
B	Sn-1Ag-0.5Cu	
C	Sn-1.2Ag-0.5Cu-0.05Ni	
D	Sn-1Ag-0.5Cu-0.05Ni	
E	Sn-1Ag-0.5Cu-0.05Ge	

combinations of five kinds of Sn-Ag-Cu solder joints, with a diameter of 500 μm, along with two kinds of substrate pad finishes, namely immersion tin (IT) and Sn-3Ag-0.5Cu direct solder on pad (DSOP). The colder compositions were conventional Sn-4Ag-0.5Cu and Sn-1Ag-0.5Cu, and three low-Ag-content Sn-Ag-Cu solder alloys doped with Ni or Ge, i.e., Sn-1Ag-0.5Cu-0.05Ni, Sn-1.2Ag-0.5Cu-0.05Ni, and Sn-1Ag-0.5Cu-0.05Ge. Note that Sn-1.2Ag-0.5Cu-0.05Ni was obtained from a supplier different from the ones that provided the other two Ni- or Ge-doped solder alloys, and hence process differences may play a role in their performance. The reflow profile for the ball mount process features a temperature increase rate of 0.8°C/s and a descending rate of 1.9°C/s, with the temperature maintained at a peak value of 260°C for 4 s. In addition to the as-mounted samples, the ten experiment sets were also subjected to reflow three more times following the same profile so that the change of the BIT responses of the solder joints with respect to multi-reflow could be examined. For each experiment cell, 20 solder joints were tested. V_i was set at 500 mm/s.

RESULTS AND DISCUSSION

The interfacial morphologies of selected intact solder joint samples with IT and DSOP substrate pad finishes are shown in Figs. 3 and 4, respectively. The interfacial IMC for all the experiment cells in this study were identified as Cu_6Sn_5 or $(Cu,Ni)_6Sn_5$ by energy-dispersive X-ray spectrometry (EDS). In the case of IT, the interfacial IMC layers of Sn-1Ag-0.5Cu and Sn-1Ag-0.5Cu-0.05Ge samples were scalloped while that of the samples with Ni addition exhibited an irregular worm-like appearance. It is assumed that Ni dissolved in the Cu_6Sn_5 layer leads to morphological changes of the layer.[18] Some discrete IMC particles distributed within the solder could be observed, with more observed in the Ni-doped solder joints. After three reflows, the thickness of the interfacial IMC appeared to increase slightly. We also noted that the DSOP finish resulted in thicker interfacial IMC layers than the IT finish for all cells. We may consider that samples with DSOP had a reduced melting point (or a lower liquidus) compared to those with IT due to the additional Sn-3Ag-0.5Cu solder paste. Consequently, the difference between the peak reflow temperature and the melting point was greater for the DSOP samples, and hence their interfacial IMC layers were thicker.

The BIT-induced fractured surfaces corresponding to modes B (IMC fracturing) and C (solder

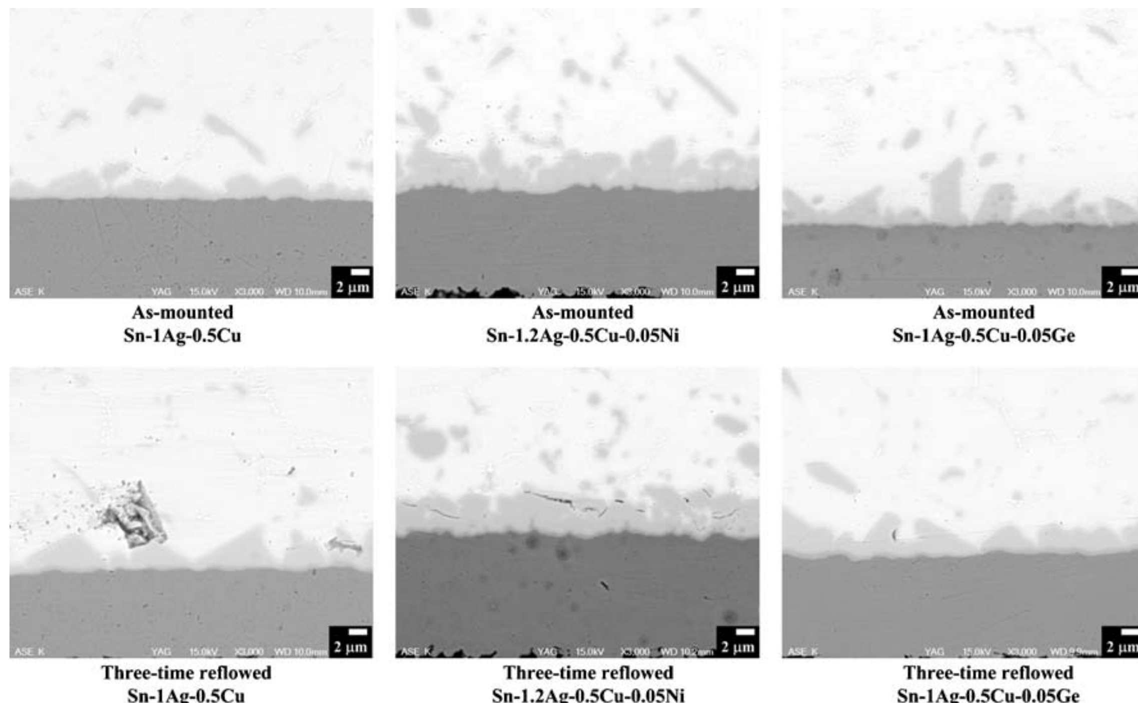

Fig. 3. Cross-sectional morphologies of intact solder joints with the IT substrate pad finish.

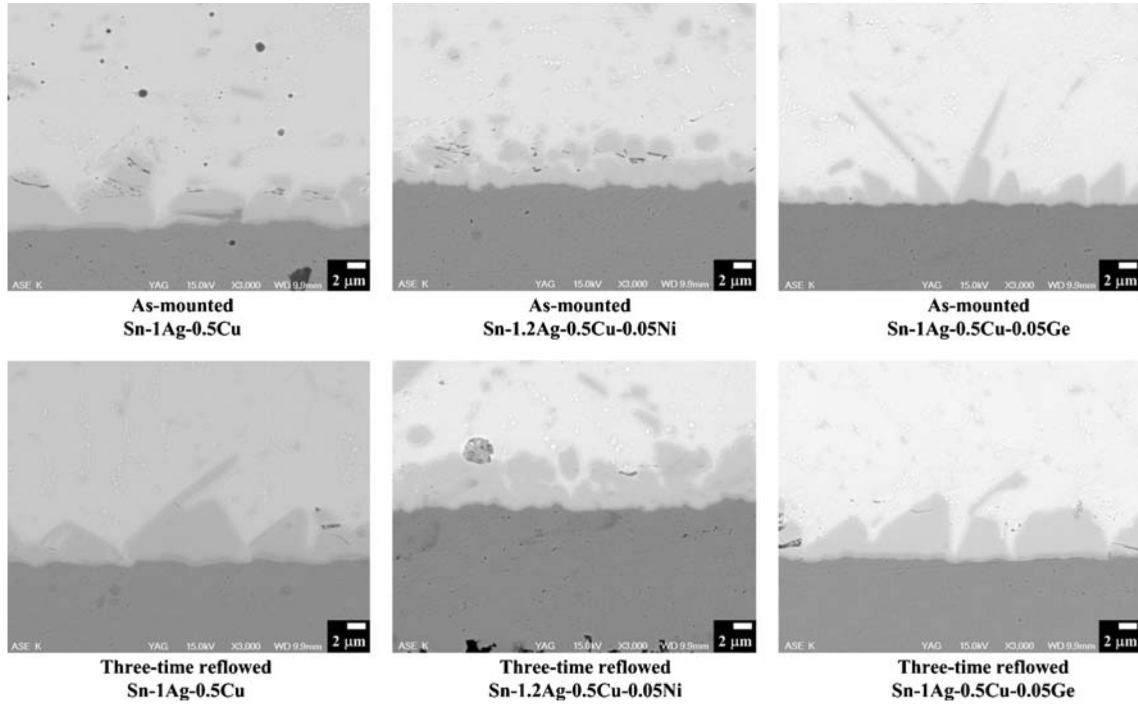

Fig. 4. Cross-sectional morphologies of intact solder joints with the DSOP substrate pad finish.

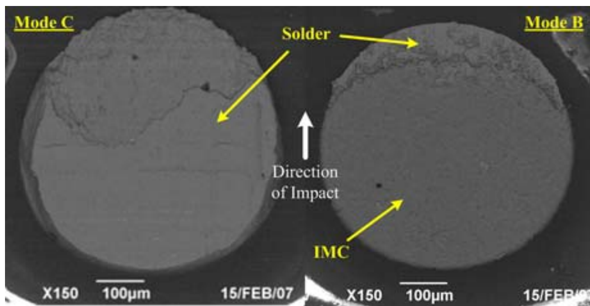

Fig. 5. Fractured surfaces corresponding to modes B and C.

fracturing) are shown in Fig. 5, in which the pin moved along the direction from bottom to top. For all the experiment cells used in this study, mode B was found to be the dominant BIT-induced failure mode while mode B1 (pad peeling) did not occur. Mode C was present only in the as-mounted Ni- or Ge-doped samples with the IT substrate pad finish: 40% (8 out of 20 solder joints) for Sn-1Ag-0.5Cu-0.05Ni with IT, and 5% (1 out of 20 solder joints) for Sn-1.2Ag-0.5Cu-0.05Ni and Sn-1Ag-0.5Cu-0.05Ge with IT. Cross-sectional examination of the fractured solder joint (Fig. 6) indicates that the BIT-induced fracture, once it has occurred around the interfacial IMC layer, propagates inside the IMC and leaves only a thin film of IMC on the surface of the Cu pad. This specific failure pattern is very similar to that caused by drop impacts in a board-level solder joint.[4,5]

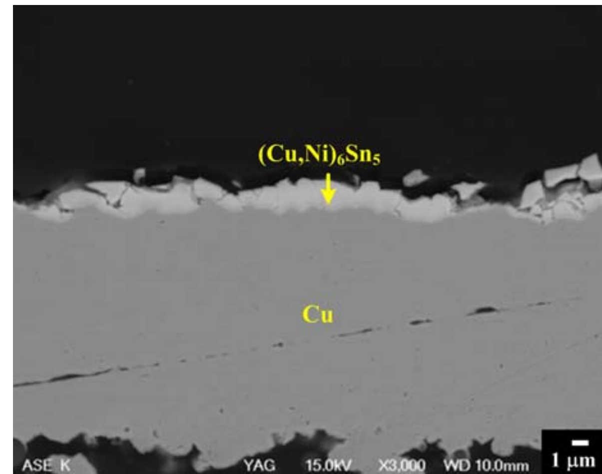

Fig. 6. Cross-sectional examinations of fractured solder joint: Sn-1.2Ag-0.5Cu-0.05Ni with the IT substrate pad finish after three reflows.

We discuss the BIT characteristics corresponding to modes B and C separately. Box plots of the measured $F_{\max}$, E_r, and δ for mode B are shown in Figs. 7–9, respectively. In a box plot, the square denotes the mean value, the box is bounded by the lower and upper quartiles, the whiskers extend to 5th and 95th percentiles, and the crosses indicate the maximum and minimum values. Apparently, these three BIT characteristics are, in general, larger for samples with the IT substrate pad finish than those with the DSOP finish. Moreover, these

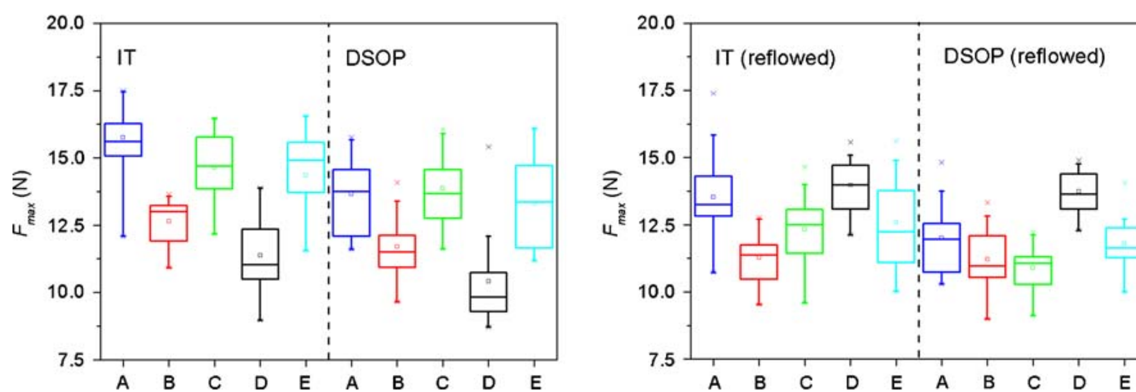

Fig. 7. F_{max} for mode B (left: as-mounted; right: reflowed three times).

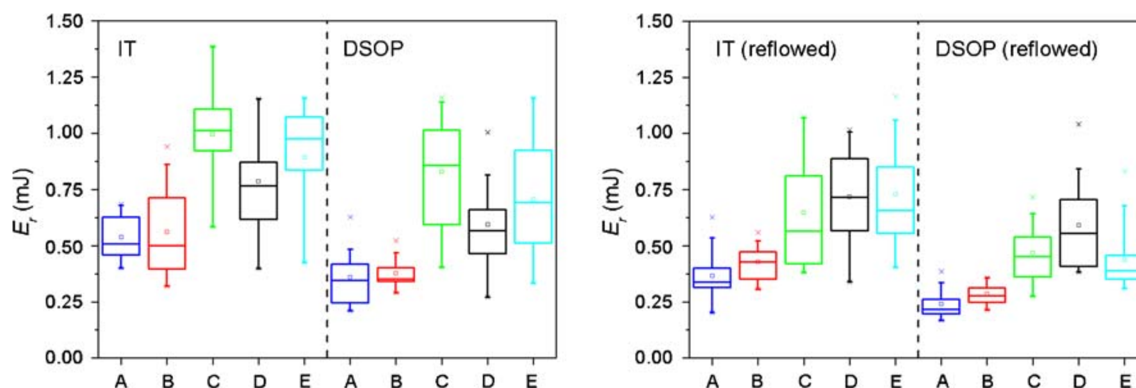

Fig. 8. E_r for mode B (left: as-mounted; right: reflowed three times).

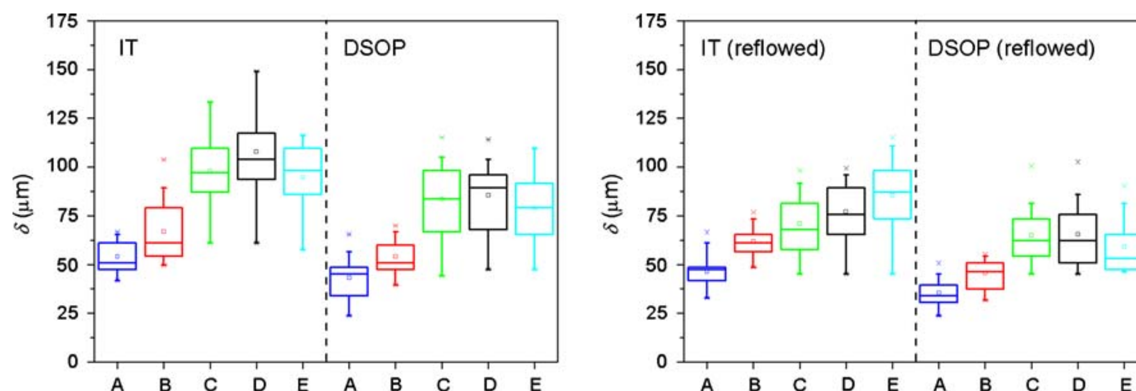

Fig. 9. δ for mode B (left: as-mounted; right: reflowed three times).

BIT characteristics for the as-mounted samples are generally higher than those for the multi-reflowed samples for all cells except for Sn-1Ag-0.5Cu-0.05Ni with IT or DSOP, for which the variation of E_r is not apparent while F_{max} increases after multi-reflow. Lai et al.[10] has pointed out that F_{max} in fact captures a combined mechanical response of the modulus, adhesion strength, and ductility of the solder joint. Therefore, the comparison of F_{max} between solder joints of different solder compositions or those subjected to different annealing or reflow conditions that lead to possible mechanical property change for the solder bulk is not particularly meaningful. Nevertheless, the increase of F_{max} with additional reflows for the Sn-1Ag-0.5Cu-0.05Ni samples remains an interesting issue that requires further investigations.

Attempts to establish an empirical correlation between board-level drop reliability and BIT characteristics have shown that physical terms related

to the impact energy, such as E_r, are more appropriate.[1,2] If this is the case, the BIT results presented in Fig. 8 imply that better board-level drop reliability can be achieved by adopting Sn-Ag-Cu solder alloys with low Ag weight contents as well as the IT rather than the DSOP substrate pad finish. Doping of the Ni or Ge trace element into the solder alloy clearly yields a great enhancement. Among the three Ni- or Ge-doped Sn-Ag-Cu solder alloys, Sn-1.2Ag-0.5Cu-0.05Ni appears to be the best, followed by Sn-1Ag-0.5Cu-0.05Ge. However, these three solder alloys would have similar performances after being reflowed three times. Also, the performance of Sn-1Ag-0.5Cu-0.05Ni does not seem to degrade after additional reflow.

Considering δ as a ductility index of the solder joint, we note from Fig. 9 that the BIT responses of the Ni- or Ge-doped Sn-Ag-Cu solder alloys are more ductile than those of conventional Sn-Ag-Cu. Among the five solder compositions examined in this study, Sn-1Ag-0.5Cu-0.05Ni is the most ductile while Sn-4Ag-0.5Cu is the most brittle. Moreover, the samples with the IT substrate pad finish exhibited more ductile responses than those with the DSOP finish. After additional reflow, the BIT responses become more brittle for all the experiment cells. Taking the diameter of the solder joint, 500 μm, as a reference, we note that IMC fracturing takes place when the pin moves a distance of about 7% (Sn-4Ag-0.5Cu with DSOP, multi-reflowed) to 20% (Sn-1Ag-0.5Cu-0.05Ni with IT, as-mounted) of the diameter.

Table II compares the BIT characteristics for modes B and C for the as-mounted Ni- or Ge-doped samples with the IT substrate pad finish, which are the only cells where mode C exists. Though the comparison is not particularly statistically meaningful because the data population for mode C is quite limited, it can be noted from the table that E_r and δ for mode C are much greater than those for mode B. This indicates that a larger energy is required for the solder joint to fracture within the solder bulk, and that solder fracturing is a more ductile process than IMC fracturing.

The BIT-induced fractographies were closely related to the solder composition. For the two undoped solder alloys, Sn-4Ag-0.5Cu and Sn-1Ag-0.5Cu, similar fractographies, as shown in Fig. 10 using Sn-4Ag-0.5Cu as an example, could be observed. Except for some Cu_6Sn_5 intermetallic islands exposed with crystalline facets, the fractured surfaces of both as-mounted and three-time reflowed specimens were flat and smooth. After three reflows, the size of the Cu_6Sn_5 exposures apparently became greater. Moreover, microcracks could be observed linking the intermetallic particles (Fig. 10c) and some scratch scars on massive intermetallics, possibly due to high-speed fracturing, were also found (Fig. 10d). Sn-Ag-Cu solder joints doped with Ni exhibited a different BIT-induced fractography. As shown in Fig. 11, the fractured surfaces of both the as-mounted and multi-reflowed Sn-1.2Ag-0.5Cu-0.05Ni solder joints were more rugged than those of the undoped ones. The intermetallic phase remained nodular after multi-reflowing and the solder matrix surrounding the intermetallics appeared to have experienced ductile deformations. Some exposed Cu-Ni-Sn particles contained a certain amount of Ni, ranging from 3 wt.% to 5 wt.%, indicating that the addition of Ni enhanced the formation of Cu-Ni-Sn particles in the liquid solder near the interface. As shown in Fig. 12, the fractographies of the Ge-containing samples were similar to those of the undoped samples, which revealed massive Cu_6Sn_5 exposures on the flat fractured surface.

The addition of Ni could be responsible for several microstructural changes such as the formation of Cu-Ni-Sn intermetallics in the solder or at the interface,[18,20,21] less packed Ag_3Sn resulted from the reduced undercooling,[21] and the morphological transition of interfacial IMCs from scalloped to worm-like.[18] With a low Ni content similar to the samples investigated in the present study, Sn-3.5Ag-0.5Cu-0.07Ni-0.01Ge shows a lower yield strength and greater elongation than Sn-3.5Ag-0.5Cu,[22] which is likely due to the less packed Ag_3Sn within the eutectic structure. When the Ni content is increased to 0.5 wt.%, Cu-Ni-Sn compounds form and somewhat suppress the effect of Ag_3Sn nodule size.[21] This causes a higher strength and degraded ductility. However, in this study, the superior BIT performance of Sn-1.2Ag-0.5Cu-0.05Ni can be mainly ascribed to the discontinuous worm-shaped Cu-Ni-Sn phase at the interface. Such interfacial IMCs may stunt crack propagation, prevent fast fracturing, and thus contribute to higher E_r and δ values, as demonstrated in Fig. 11 by the ductile deformed Sn matrix on the rugged fractured surface. For Ge, Chuang et al.[18] suggested that it was not involved in the interfacial reaction and thus the morphology of interfacial Cu_6Sn_5 was not significantly altered compared to undoped Sn-Ag-Cu samples. Therefore, the improved BIT performance through minor Ge alloying might be related to its positive effect on the mechanical behavior of the bulk solder.

Table II. Comparison of BIT Characteristics for Modes B and C

As-Mounted Cell with the IT Pad Finish	F_{max} (N)	E_r (mJ)	δ (μm)
C (mode B)	14.66 ± 1.26	1.00 ± 0.18	98.0 ± 16.4
D (mode B)	11.68 ± 1.67	0.80 ± 0.21	108.4 ± 22.8
E (mode B)	14.31 ± 1.59	0.86 ± 0.28	92.6 ± 20.8
C (mode C)	16.76	2.14	161.6
D (mode C)	16.77 ± 1.08	1.40 ± 0.40	113.4 ± 30.3
E (mode C)	16.81	2.10	176.2

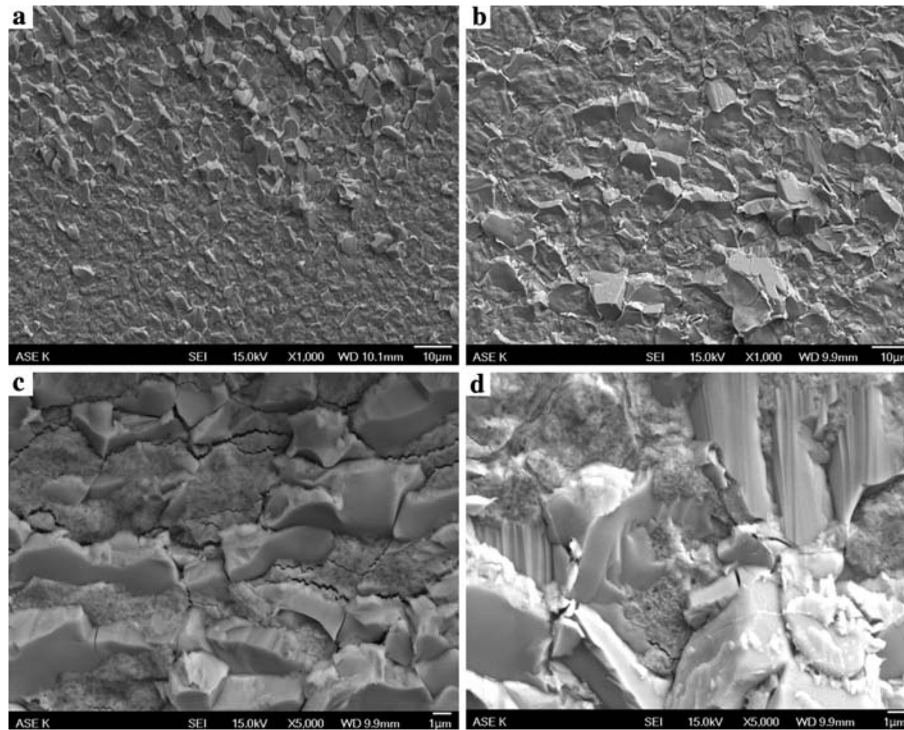

Fig. 10. Fractographies of the Sn-4Ag-0.5Cu solder joint with the IT substrate pad finish: (a) as-mounted, (b) three-time reflowed, (c) and (d) enlarged microstructures of (b).

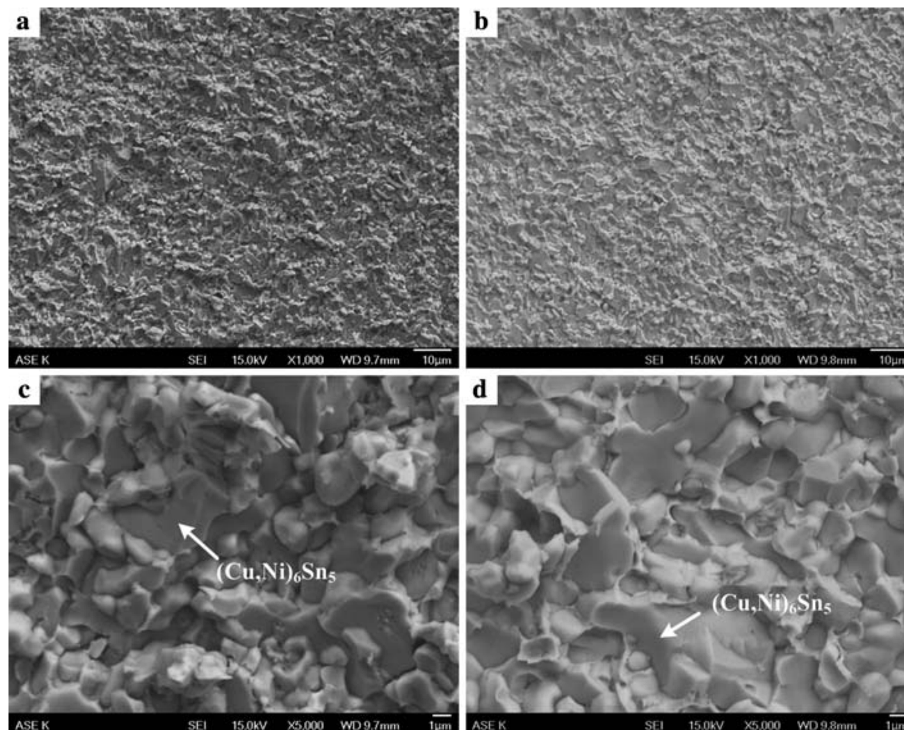

Fig. 11. Fractographies of the Sn-1.2Ag-0.5Cu-0.05Ni solder joint with the IT substrate pad finish: (a) as-mounted, (b) three-time reflowed, (c) and (d) enlarged microstructures of (a) and (b), respectively.

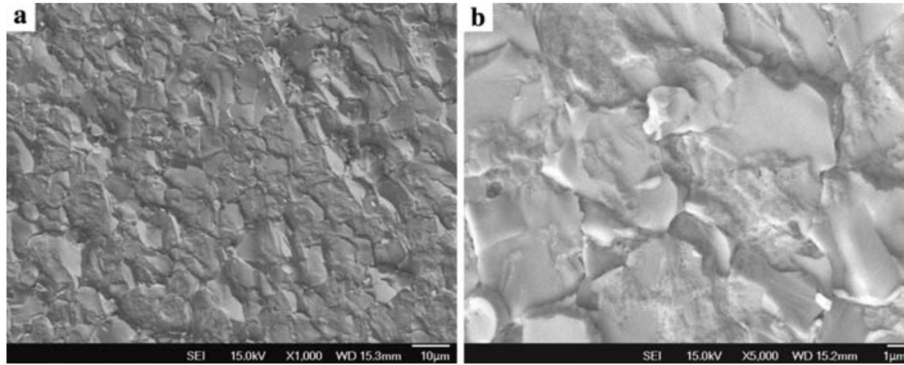

Fig. 12. Fractographies of the Sn-1Ag-0.5Cu-0.05Ge solder joint with the IT substrate pad finish: (a) three-time reflowed and (b) enlarged microstructures of (a).

CONCLUSIONS

We present BIT characteristics measured at an impact velocity of 500 mm/s for Sn-4Ag-0.5Cu, Sn-1Ag-0.5Cu, Sn-1Ag-0.5Cu-0.05Ni, Sn-1.2Ag-0.5Cu-0.05Ni, and Sn-1Ag-0.5Cu-0.05Ge package-level solder joints, bonded on substrate pads with IT and DSOP surface finishes. The effect of multi-reflow on the variation of BIT responses was also examined.

For all the experiment cells investigated in this study, IMC fracturing was found to be the dominant BIT-induced failure mode. Solder fracturing was present only in the as-mounted Ni- or Ge-doped samples with the IT substrate pad finish. The BIT characteristics were greater for samples with the IT substrate pad finish than those with the DSOP finish. Also, the BIT characteristics for as-mounted samples were greater than those for the multi-reflowed samples for all cells except for Sn-1Ag-0.5Cu-0.05Ni, for which the variation of E_r is not apparent while F_{max} increases after multi-reflow.

Taking E_r as an indication for board-level drop reliability, we note from the BIT results that better board-level drop reliability can be achieved by adopting Sn-Ag-Cu solder alloys with low Ag weight contents as well as the IT rather than the DSOP substrate pad finish. Moreover, the addition of Ni or Ge to the solder alloy yields a great enhancement; Ni alters the interfacial IMC structure while Ge enhances the mechanical behavior of the bulk solder.

The BIT responses of Ni- or Ge-doped Sn-Ag-Cu solder alloys are more ductile than those of conventional Sn-Ag-Cu. Among the five solder compositions examined in this study, Sn-1Ag-0.5Cu-0.05Ni was the most ductile while Sn-4Ag-0.5Cu was the most brittle. Samples with the IT substrate pad finish had more ductile responses than those with the DSOP finish. After additional reflow, all experiment cells exhibit more brittle BIT responses. Moreover, a larger energy is required for the solder joint to fracture within the solder bulk, and solder fracturing is a more ductile process than IMC fracturing.

ACKNOWLEDGEMENTS

The authors are grateful to Dr. Chang-Lin Yeh for technical comments and Shu-Hsien Lee and Chiu-Wen Lee for experimental support.

REFERENCES

1. E.H. Wong, R. Rajoo, Y.-W. Mai, S.K.W. Seah, K.T. Tsai, and L.M. Yap, *Proceedings of the 55th Electronic Components and Technology Conference* (Piscataway, NJ: IEEE, 2005), p. 1202.
2. C.-L. Yeh, Y.-S. Lai, H.-C. Chang, and T.-H. Chen, *Microelectron. Reliab.* 47, 1127 (2007).
3. Y.-S. Lai, P.-F. Yang, and C.-L. Yeh, *Microelectron. Reliab.* 46, 645 (2006).
4. D.Y.R. Chong, F.X. Che, J.H.L. Pang, K. Ng, J.Y.N. Tan, and P.T.H. Low, *Microelectron. Reliab.* 46, 1160 (2006).
5. Y.-S. Lai, P.-C. Yang, and C.-L. Yeh, *Microelectron. Reliab.* doi: 10.1016/j.microrel.2007.03.005.
6. M. Date, T. Shoji, M. Fujiyoshi, K. Sato, and K.N. Tu, *Scripta Mater.* 51, 641 (2004).
7. K. Newman, *Proceedings of the 55th Electronic Components and Technology Conference* (Piscataway, NJ: IEEE, 2005), p. 1194.
8. J.Y.H. Chia, B. Cotterell, and T.C. Chai, *Mater. Sci. Eng.: A* 417, 259 (2006).
9. Y.-S. Lai, C.-L. Yeh, H.-C. Chang, and C.-L. Kao, *J. Alloy. Comp.* doi: 10.1016/j.jallcom.2006.10.102.
10. Y.-S. Lai, H.-C. Chang and C.-L. Yeh, *Microelectron. Reliab.* 47, 2179 (2007).
11. C.-L. Yeh and Y.-S. Lai, *J. Electron. Packag.* 129, 98 (2007).
12. C.-L. Yeh, Y.-S. Lai, and P.-F. Yang, *Proceedings of the 9th IMAPS Topical Workshop on Flip Chip Technologies* (Washington, DC: IMAPS, 2004).
13. C.-L. Yeh and Y.-S. Lai, *Microelectron. Reliab.* 46, 885 (2006).
14. C.-L. Yeh and Y.-S. Lai, *J. Electron. Mater.* 35, 1892 (2006).
15. C.-L. Yeh and Y.-S. Lai, *IEEE Trans. Electron. Packag. Manuf.* 30, 84 (2007).
16. Y. Kariya, T. Hosoi, S. Terashima, M. Tanaka, and M. Otsuka, *J. Electron. Mater.* 33, 321 (2004).
17. Y. Kariya, T. Hosoi, T. Kimura, S. Terashima, M. Tanaka, and T. Suga, *Proceedings of the 9th Intersociety Conference on Thermal and Thermomechanical Phenomena in Electronic Systems* (Piscataway, NJ: IEEE, 2004), p. 103.
18. C.-M. Chuang and K.-L. Lin, *J. Electron. Mater.* 32, 1426 (2003).
19. K. Habu, N. Takeda, H. Watanabe, H. Ooki, J. Abe, T. Saito, Y. Taniguchi, and K. Takayama, *Proceedings of EcoDesign: 1st International Symposium on Environmentally Conscious*

Design and Inverse Manufacturing (Piscataway, NJ: IEEE, 1999), p. 606.
20. J.W. Lee, Z.H. Lee, and H.M. Lee, *Mater. Trans.* 46, 2344 (2005).
21. J.-M. Song, C.-F. Huang, and H.-Y. Chuang, *J. Electron. Mater.* 35, 2154 (2006).
22. C.-M. Chuang, P.-C. Shih, and K.-L. Lin, *J. Electron. Mater.* 33, 1 (2004).